Acta Neurochir
DOI 10.1007/s00701-010-0636-3

CLINICAL ARTICLE

Mechanisms of cerebellar tonsil herniation in patients with Chiari malformations as guide to clinical management

Thomas H. Milhorat · Misao Nishikawa · Roger W. Kula · Yosef D. Dlugacz

Received: 12 January 2010 / Accepted: 11 March 2010

Abstract
Background The pathogenesis of Chiari malformations is incompletely understood. We tested the hypothesis that different etiologies have different mechanisms of cerebellar tonsil herniation (CTH), as revealed by posterior cranial fossa (PCF) morphology.
Methods In 741 patients with Chiari malformation type I (CM-I) and 11 patients with Chiari malformation type II (CM-II), the size of the occipital enchondrium and volume of the PCF (PCFV) were measured on reconstructed 2D-CT and MR images of the skull. Measurements were compared with those in 80 age- and sex-matched healthy control individuals, and the results were correlated with clinical findings.
Results Significant reductions of PCF size and volume were present in 388 patients with classical CM-I, 11 patients with CM-II, and five patients with CM-I and craniosynostosis. Occipital bone size and PCFV were normal in 225 patients with CM-I and occipitoatlantoaxial joint instability, 55 patients with CM-I and tethered cord syndrome (TCS), 30 patients with CM-I and intracranial mass lesions, and 28 patients with CM-I and lumboperitoneal shunts. Ten patients had miscellaneous etiologies. The size and area of the foramen magnum were significantly smaller in patients with classical CM-I and CM-I occurring with craniosynostosis and significantly larger in patients with CM-II and CM-I occurring with TCS.
Conclusions Important clues concerning the pathogenesis of CTH were provided by morphometric measurements of the PCF. When these assessments were correlated with etiological factors, the following causal mechanisms were suggested: (1) cranial constriction; (2) cranial settling; (3) spinal cord tethering; (4) intracranial hypertension; and (5) intraspinal hypotension.

Keywords Chiari malformation · Cerebellar tonsil herniation · Posterior cranial fossa · Foramen magnum · Skull base hypoplasia

T. H. Milhorat
Feinstein Institute for Medical Research,
North Shore-Long Island Jewish Health System,
Manhasset,
New York, USA

T. H. Milhorat · M. Nishikawa · R. W. Kula
The Chiari Institute,
North Shore-Long Island Jewish Health System,
Great Neck,
New York, USA

Y. D. Dlugacz
Krasnoff Quality Management Institute,
North Shore-Long Island Jewish Health System,
Great Neck,
New York, USA

R. W. Kula
Department of Neurology,
North Shore-Long Island Jewish Health System,
Manhasset,
New York, USA

T. H. Milhorat · M. Nishikawa
Department of Neurosurgery,
North Shore-Long Island Jewish Health System,
Manhasset,
New York, USA

T. H. Milhorat (✉)
The Chiari Institute,
865 Northern Blvd., Suite 302, Great Neck,
New York 11021-5310, USA
e-mail: Milhorat@nshs.edu

Published online: 04 May 2010

Abbreviations

2D-CT	two-dimensional computerized tomography
CM-I	Chiari malformation type I
CM-II	Chiari malformation type II
CTH	cerebellar tonsil herniation
FM	foramen magnum
FT	filum terminale
HDCT	hereditary disorders of connective tissue
MRI	magnetic resonance imaging
MASS	mitral valve prolapse, aortic anomalies, skeletal changes, and skin changes
OAAJI	occipitoatlantoaxial joint instability
PCF	posterior cranial fossa
PCFV	posterior cranial fossa volume
PCFV-ATL	posterior cranial fossa volume above Twining's line
PCFV-BTL	posterior cranial fossa volume below Twining's line
PFBV	posterior fossa brain volume
SD	standardized deviation
SPSS	Statistical Package for the Social Science
TCS	tethered cord syndrome

Introduction

Cerebellar ectopia is a relatively common magnetic resonance imaging (MRI) finding. Chiari malformation type I (CM-I) is defined radiographically as a simple displacement of the cerebellar tonsils 5 mm or greater below the foramen magnum (FM) [8] and is distinguished from the less common Chiari malformation type II (CM-II) occurring with myelodysplasia and the rare Chiari malformation type III (CM-III) occurring with cervical encephalocele [4]. Whereas CM-II and CM-III are gross defects of neuroectodermal origin, there is accumulating evidence that CM-I is a disorder of the paraaxial mesoderm that results in underdevelopment of the posterior cranial fossa (PCF) and overcrowding of the hindbrain [19, 25, 30]. However, CM-I can also occur in association with disorders that appear to be unrelated to skull base hypoplasia such as hydrocephalus [4], intracranial mass lesions [12, 22], cerebrospinal fluid (CSF) leaks [2], prolonged lumboperitoneal shunting [5], hereditary disorders of connective tissue (HDCT) associated with occipitoatlantoaxial joint instability (OAAJI) and cranial settling [20], tethered cord syndrome [19], and miscellaneous conditions such as craniosynostosis [6], acromegaly [13], and Paget's disease [7]. This raises the possibility that generically defined CM-I may have more than one causal mechanism.

In the current study, morphometric assessments of the PCF were correlated with clinical findings in 752 patients with Chiari malformations. When the data were stratified according etiological factors, five distinct mechanisms of cerebellar tonsil herniation (CTH) were identified that appear to have diagnostic and therapeutic implications.

Methods

Patient population

The study population was selected from a database of 3,318 patients with Chiari malformations who were evaluated consecutively between January 2002 and December 2008. Inclusion criteria were limited to clinically symptomatic patients between the ages of 15–69 years who had one or more disabling symptoms, complete neuroimaging of the head and spine, and no prior Chiari-related surgery. For clarity and focus, all patients met the unambiguous and widely accepted radiographic criteria of tonsillar descent (≥5 mm) below the FM. Patients younger than 15 years and older than 69 years were excluded to minimize age-related changes of the skull and brain [29]. There were 545 females and 207 males with a mean age of 32.7 years (±11.0 SD).

Assessment tools

We used the database (Microsoft Access 2007) of a clinical research repository that included detailed information about the medical history, family history, symptoms and signs, and genetic associations of patients with Chiari malformations and related disorders. All patients had undergone a physical examination, complete neurological examination, measurement of articular mobility, whole neuraxis MRI, and 3D-CT scans of the head and upper cervical spine with two-dimensional computerized tomography (2D-CT) reconstructions. Additional information was provided in some patients by Cine-MRI, upright MRI, flexion and extension X-rays of the cervical spine, cervical traction tests [20], and CT scans of the lumbosacral spine.

Diagnostic criteria

The diagnosis of CM-I was made using the narrow but widely accepted radiographic definition of descent of the cerebellar tonsils 5 mm or greater below the FM [8]. CM-I with no etiological cofactors was defined as classical CM-I. The diagnosis of CM-II was based on radiographic evidence of cerebellar tonsillar herniation in association with spina bifida, myelodysplasia, and associated neuroectodermal defects. Diagnostic criteria for HDCT have been published previously [20, 27]. Radiographic criteria for OAAJI and cranial settling in patients with either HDCT or posttraumatic craniocervical instability included evidence

of atlantoaxial and/or atlantooccipital joint hypermobility with posterior gliding of the occipital condyles and cranial settling (≥3 mm) upon assumption of the upright position [20]. The diagnosis of TCS was limited to patients who met the following criteria: (1) low position of the conus medullaris (at or below the $L_{2–3}$ interspace); (2) thickening (<2.0 mm diameter) and/or fatty infiltration of the filum terminale (FT); and (3) typical TCS symptomatology [14, 19, 28].

Morphometric analysis of the posterior cranial fossa

All morphometric and volumetric measurements were by a single experienced observer (MN) who was unaware of other study data. Linear measurements were made to accuracy of 0.1 mm as determined by calibrated computer software. The results were reviewed independently by two experienced observers who oversaw the process and verified the calculations. Normative data were obtained from randomly selected, standardized radiographic images in age- and sex-matched individuals who had no identifiable clinical or radiographic abnormalities.

Using reconstructed 2D-CT and MRI scans of the head, the size of the occipital bone was determined by measuring its enchondral parts (exocciput, basiocciput, and supraocciput), which enclose the PCF (Fig. 1) [21, 24, 25]. Measurements included the axial length of the clivus (basiocciput and basisphenoid) from the top of the dorsum sella to the basion; the axial length of the supraocciput from the center of the internal occipital protuberance to the opisthion; the axial length of the occipital condyle (exocciput) from the top of the jugular tubercle to the bottom of the occipital condyle [19, 25]; and the widths of the clivus (distance between the bilateral carotid canals), the supraocciput (distance between the inner surfaces of the asterions), and the occipital condyles (distance between the outer surfaces of the condyles) [19, 25]. The anterior–posterior diameter of the FM was measured as the distance between the inner surfaces of the basion and opisthion on midsaggital reconstructed 2D-CT images. The transverse diameter (width) of the FM was measured as the maximal interval between the inner surfaces of the occipital condyles on axial reconstructed 2D-CT images. Radiographic analysis software (Rasband, W.S., ImageJ, National Institutes of Health, Bethesda, MD, USA, 1997–2008) was used to calculate the area of the FM at 2 levels: (1) the inferior outlet between the basion and opisthion and (2) the superior outlet at the level of the jugular tubercles.

Volumetric analysis of the posterior cranial fossa

The PCF was defined as the almost circular space bounded by the tentorium cerebelli, occipital bone, clivus, petrous bone, and petrous ridges [21, 25]. The ridges of the petrous

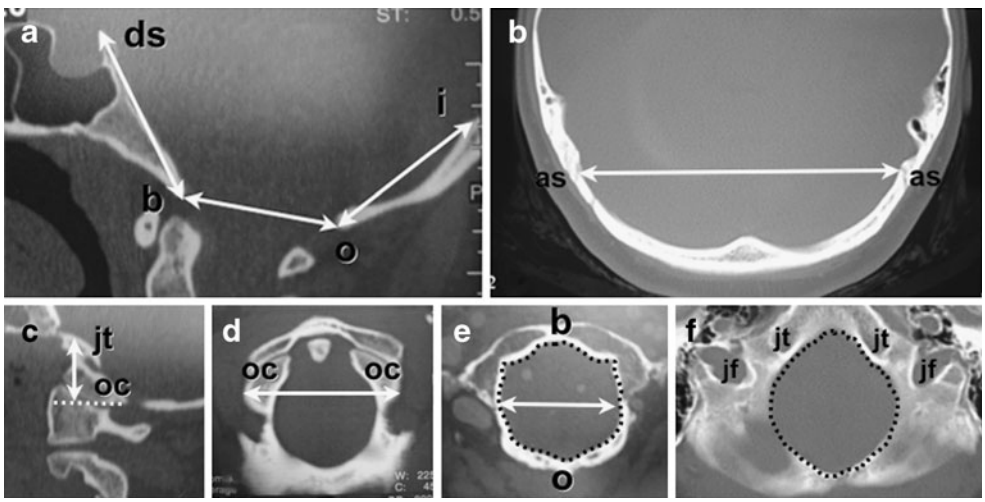

Fig. 1 Morphometric analysis of PCF using reconstructed 2D-CT images in 25-year-old healthy control female. The size of the occipital bone was determined by measuring its enchondral parts (exocciput, basiocciput, and supraocciput) which enclose the posterior cranial fossa. **a** Axial length of clivus (basiocciput and basisphenoid) measured from the top of the dorsum sellae (*ds*) to the basion (*b*); axial length of supraocciput measured from the center of the internal occipital protuberance (*i*) to the opisthion (*o*); and anterior–posterior diameter of foramen magnum measured as the distance between the inner surfaces of the basion and opisthion on midsaggital images. **b** Width of supraocciput measured as the distance between the inner surfaces of the asterions (*as*). **c** The axial height of occipital condyle (exocciput) was measured as the perpendicular distance between the top of the jugular tubercle (*jt*) and the bottom of the occipital condyle (*oc*) along a line parallel with the orbitomeatal line. **d** The width of the occipital condyles (*oc*) was measured as the distance between their outer surfaces. **e** The maximum transverse diameter of the inferior outlet of the foramen magnum was measured at the level of the basion (*b*) and opisthion (*o*). The area of the inferior outlet of the foramen magnum is enclosed by *dotted line*. **f** The area of the superior outlet of the foramen magnum was measured at level of the jugular tubercles (*jt*) and jugular foramina (*jf*) and is enclosed by *dotted line*

bones form the anterolateral border of the cavity, and their connection to the posterior clinoids (posterior petroclinoid ligament) forms the anterior border. The posterior fossa brain volume (PCBV) was defined as the neural contents of the PCF including the cerebellum, mesencephalon, pons, and medulla. Volumetric calculations were performed using radiographic analysis software (ImageJ) and the Cavalieri method [16, 21]. The PCFV was calculated on reconstructed 2D-CT images, and the PCBV were calculated on MRI axial and sagittal images, excluding the fourth ventricle and including the herniated cerebellar tonsils and medulla. PCFV was divided into the volume above Twining's line (PCFV-ATL) and below Twining's line (PCFV-BTL). The volume of the CSF spaces was calculated as the PCFV minus PFBV.

Statistical analysis

Statistical analyses were performed with SPSS for Windows (version 15.0, SPSS Inc., Chicago, IL). Mean values are presented as ±1 SD in groups having Gaussian distribution. Median values are presented with ranges in groups having non-Gaussian distribution. The distribution of data was analyzed using the F-test. Significance was indicated by a two-tailed P value of less than 0.01. Demographic differences between patients and healthy control individuals were tested with the nonparametric Mann-Whitney U-test and either the Student's t test for unequal sample sizes and equal variance or Welch's t test for individuals of unequal sample sizes and unequal variance by F-test. Data were divided into the following subgroups: (1) classical CM-I with no etiological cofactors; (2) CM-I associated with OAAJI and cranial settling; (3) CM-I associated with TCS; (4) CM-I associated with hydrocephalus and/or intracranial mass lesions; (5) CM-I associated with lumboperitoneal shunts; (6) CM-I associated with craniosynostosis; (7) CM-I associated with miscellaneous disorders; and (8) CM-II.

Results

The results of morphometric analysis of the PCF in patients with Chiari malformations are given in Tables 1 and 2. Table 3 summarizes morphometric distinctions according to etiology. The ranges of PFCV and FM outlet area are given in Figs. 2 and 3, respectively. Figure 4 shows variations of FM morphology.

Classical CM-I

In 388 patients with classical CM-I, diagnostic findings were limited to those known to occur with this disorder. Morphometric analysis of the PCF revealed significant reductions of occipital bone size including decreased axial lengths of the supraocciput ($P<0.001$), clivus ($P<0.001$), and occipital condyles ($P<0.001$). The FM was characteristically small with reductions of the transverse diameter ($P<0.001$), inferior outlet area ($P<0.001$), and superior outlet area ($P<0.001$). Volumetric calculations revealed a significant reduction of PCFV-BTL ($P<0.001$), enlargement of PCFV-ATL ($P<0.001$), and an overall reduction of PCFV ($P<0.001$).

CM-I and cranial settling

CM-I was associated with OAAJI and cranial settling in 52 patients with craniocervical trauma and 173 patients with the following HDCT: Ehlers–Danlos syndrome (130 patients); Marfan syndrome (nine patients); MASS (mitral valve prolapse, aortic anomalies, skeletal changes, and skin changes) phenotype (five patients); and overlap phenotype disorder (29 patients). The large number of patients with this concurrence was biased by referral patterns [20]. Clinical distinctions included a predominance of lower brain stem symptomatology, odontoid pannus formation with basilar impression, and radiographic evidence of cranial settling [20]. Morphometric analysis of the PCF in this cohort revealed normal occipital bone size, normal PCFV, normal size and area of the FM, and normal PFBV.

CM-I and tethered cord syndrome

CM-I was associated with TCS and a low-lying conus medullaris in 55 patients. Morphometric analysis of the PCF revealed no differences in occipital bone size, PCFV, and PFBV as compared with healthy control individuals. The FM was characteristically large with increases of the transverse diameter ($P<0.001$), antero-posterior diameter ($P<0.001$), inferior outlet area ($P<0.001$), and superior outlet area ($P<0.001$).

CM-I and space-occupying intracranial lesions

In 30 patients, CM-I was associated with a space-occupying intracranial lesion that presented with symptoms and signs of raised intracranial pressure and/or radiographic evidence of cerebral or cerebellar displacement. The lesions included: hydrocephalus (21 patients); arachnoid cysts of the posterior fossa (five patients); chronic subdural hematoma (one patient); falx meningioma (one patient); clivus meningioma (one patient); and acoustic neuroma (one patient). Morphometric analysis of the PCF revealed no significant differences in occipital bone size, PCFV, size and area of the FM, and PFBV as compared with healthy control individuals.

Table 1 Morphometric analysis of the posterior cranial fossa in patients with cerebellar tonsil herniation stratified according to etiology

Variable	Normal controls	CM-I	CM-I/OAAJI	CM-I/TCS
Total no. cases	80	388 (52%)	225 (30%)	55 (7%)
Male/female	25/55	111/277	44/181	15/40
Mean age (years)	31.7±11.8	33.6±10.1	31.4±10.7	30.1±11.4
Occipital bone size				
Clivus				
Axial length (mm)	47.0±2.17	38.4±3.27 (<0.001)	45.7±3.11	46.1±3.24
Distance between carotid canals (mm)	20.4±1.86	18.0±3.02 (<0.001)	20.2±2.28	20.5±2.40
Supraocciput				
Axial length (mm)	47.7±2.52	39.6±3.87 (<0.001)	46.8±3.23	47.0±2.77
Distance between asterions (mm)	101.8±3.73	96.8±3.18 (<0.001)	100.5±6.34	102.3±8.47
Condyle				
Axial height right (mm)	24.1±1.75	18.7±3.51 (<0.001)	23.7±2.87	23.6±2.65
Axial height left (mm)	24.3±1.54	19.1±3.87 (<0.001)	23.8±3.01	24.0±2.78
Width of condyles (mm)	50.5±2.48	46.8±3.69 (0.007)	50.5±4.33	55.2±2.74 (<0.001)
Foramen magnum				
Anterior–posterior diameter (mm)	32.5±3.17	32.1±3.72	33.2±2.63	37.4±2.41 (< 0.001)
Transverse diameter (mm)	30.8±3.74	26.7±3.12 (<.001)	30.8±2.78	35.1±2.71 (<0.001)
Inferior outlet area (mm^2)	787.7±118.4	651.7±121.8 (<0.001)	802.7±131.6	1,000.4±123.8 (<0.001)
Superior outlet area (mm^2)	1,774.2±128.2	1,523.5±125.7 (<0.001)	1,756.5±124.5	2,001.3±127.4 (<0.001)
Volumetric analysis				
PCFV (ml)	190.1±7.84	165.8±8.17 (<0.001)	188.2±7.78	188.0±8.72
PCFV-ATL (ml)	44.5±5.22	48.1±4.84 (<0.001)	44.7±4.96	45.2±5.35
PCFV-BTL (ml)	145.7±4.88	117.6±8.65 (<0.001)	143.5±7.40	142.8±7.20
PFBV (ml)	151.8±3.14	148.7±4.77	149.7±4.77	150.5±4.48

Numbers in parentheses denote *P* values. Results are expressed as mean values±1 SD. Abbreviations: *CM-I* Chiari malformation type I, *OAAJI* occipitoatlantoaxial joint instability, *TCS* tethered cord syndrome, *PCFV* posterior cranial fossa volume, *ATL* above Twining's line, *BTL* below Twining's line, *PFBV* posterior fossa brain volume

CM-I and lumboperitoneal shunt

CM-I was present in 28 patients with a lumboperitoneal shunt that had been implanted as treatment for pseudotumor cerebri or hydrocephalus 5 months to 16 years (mean= 2.2 years, ±1.87 SD) prior to morphometric analysis. The functional status of the shunts and the position of the cerebellar tonsils prior to shunting were not investigated. Measurements of the PCF in this cohort revealed normal occipital bone size, normal PCFV, normal size and area of the FM, and normal PFBV.

CM-I and craniosynostosis

An association of CM-I and premature stenosis of the cranial sutures was present in two patients with Crouzon's syndrome, one patient with Apert's syndrome, and two patients with nonsyndromic craniosynostosis. In this cohort, morphometric analysis of the PCF revealed significant reductions of occipital bone size including decreased axial lengths of the supraocciput ($P<0.001$), clivus ($P<0.001$), and occipital condyles ($P<0.001$). The FM was characteristically small with reductions of the anterior–posterior diameter ($P<0.001$), transverse diameter ($P<0.001$), inferior outlet area ($P<0.001$), and superior outlet area ($P<0.001$). Volumetric calculations revealed a reduction of PCFV below Twining's line ($P<0.001$), normal PCFV above Twining's line, and an overall reduction of PCFV ($P<0.001$) as compared with healthy control individuals. PFBV was normal.

CM-I and miscellaneous cases

Morphometric assessments of the PCF were made in ten patients with CM-I and miscellaneous disorders. Reductions of occipital bone size, PCFV, and FM size and area that exceeded 2 SD were present in four of four patients with achondroplasia, two of two patients with acromegaly, and one of one patient with Paget's disease. In three of three patients with osteogenesis imperfecta, occipital bone size, PCFV, and FM size and area were within 1 SD of normal. These data were not statistically significant owing to small sample size.

Table 2 Morphometric analysis of the posterior cranial fossa in patients with cerebellar tonsil herniation stratified according to etiology

Variable	CM-I/ISOL	CM-I/LPS	CM-I/CS	CM-II
Total no. cases	30 (4%)	28 (4%)	5 (1%)	11 (1%)
Male/female	12/18	12/16	2/3	5/6
Mean age (years)	38.7±17.5	39.5±16.4	18.3:16–21	25.1:16–34
Occipital bone size				
Clivus				
Axial length (mm)	47.1±2.24	47.5±2.55	36.5:31.4–41.5 (<0.001)	38.0:32.0–44.1 (<0.001)
Distance between carotid canals (mm)	20.5±2.11	20.6±2.04	16.2:12.7–18.8 (<0.001)	15.8:11.8–19.6 (0.004)
Supraocciput				
Axial length (mm)	47.5±2.72	47.8±3.24	41.5:39.3–43.5 (<0.001)	38.7:30.1–46.9 (<0.001)
Distance between asterions (mm)	101.3±8.25	100.5±4.54	96.5:91.5–101.7 (0.003)	92.5:87.2–97.8 (<0.001)
Condyle				
Axial height right (mm)	25.1±2.88	25.4±2.73	16.8:12.1–21.0 (<0.001)	18.5:11.0–25.6 (<0.001)
Axial height left (mm)	24.8±2.76	25.2±3.12	17.8:14.7–22.0 (0.002)	18.7:11.2–25.4 (<0.001)
Width of condyles (mm)	50.1±3.77	50.3±3.43	46.1:41.8–50.5 (0.01)	58.7:51.9–56.1 (<0.001)
Foramen magnum				
Anterior–posterior diameter (mm)	32.7±3.51	31.8±3.57	28.5:21.7–39.8 (0.007)	39.3:32.6–46.7 (<0.001)
Transverse diameter (mm)	29.6±3.43	29.6±2.96	27.3:20.4–34.3 (0.01)	36.8:29.1–44.7 (<0.001)
Inferior outlet area (mm^2)	772.5±128.7	741.4±126.2	615.9:584–648 (0.008)	1,077.1:887–1,171 (<0.001)
Superior outlet area (mm^2)	1,725±122.7	1,721±124.2	1,502:1,318–1,657 (0.002)	1,972.4:1,804–2,137 (<0.001)
Volumetric analysis				
PCFV (ml)	190.1±8.12	189.5±5.12	165.3:148.2–181.7 (<0.001)	161.5:142.0–173.4 (<0.001)
PCFV-ATL (ml)	44.8±4.85	42.7±1.71	43.3:39.1–47.5	33.7:25.0–43.4 (<0.001)
PCFV-BTL (ml)	145.2±4.77	146.8±11.1	122.0:114.7–129.5 (<0.001)	127.7:118.7–136.9 (<0.001)
PFBV (ml)	154.7±8.12	150.8±3.76	148.0:140.7–155.8	147.1:140.8–155.2

Numbers in parentheses denote *P* values. Results are expressed as mean values±1 SD in patients with CM-I/ISOL and CM-I/LPS. In patients with CM-I/CS and CM-II, results are expressed as median values with ranges owing to non-Gaussian distribution. Abbreviations: *CM-I* Chiari malformation type I, *ISOL* intracranial space-occupying lesions, *LPS* lumboperitoneal shunt, *CS* craniosynostosis, *CM-II* Chiari malformation type II, *PCFV* posterior cranial fossa volume, *ATL* above Twining's line, *BTL* below Twining's line, *PFBV* posterior fossa brain volume

Chiari II malformation

CM-II occurring in association with myelomeningocele and related neuroectodermal defects was present in 11 patients with no prior cranial surgery except for implantation and revision of ventriculoperitoneal shunts. None of the patients had ventriculomegaly at the time of morphometric analysis. Assessments of the PCF revealed significant reductions of occipital bone size including the axial length and width of the clivus ($P<0.001$ and $P<0.004$, respectively), the axial length of the supraocciput ($P<0.001$), and the axial length and width of the occipital condyles ($P<0.001$). The foramen magnum was characteristically large with increases of the anterior–posterior diameter ($P<0.001$), transverse diameter ($P<0.001$), inferior outlet area ($P<0.001$), and superior outlet area ($P<0.001$). Volumetric calculations revealed reductions of the PCFV ($P<0.001$) both above and below Twining's line ($P<0.001$) as

Table 3 Summary of posterior cranial fossa morphology in patients with Chiari malformations stratified according to etiology

	Occipital bone size	PCFV	FM
CM-I (classical type)	Small	Small	Small
CM-I/craniosynostosis	Small	Small	Small
CM-II/(with myelodysplasia)	Small	Small	Large
CM-I/tethered cord syndrome	Normal	Normal	Large
CM-I/cranial settling	Normal	Normal	Normal
CM-I/intracranial space-occupying lesions	Normal	Normal	Normal
CM-I/lumboperitoneal shunt	Normal	Normal	Normal

Abbreviations: *PCFV* posterior cranial fossa volume, *FM* foramen magnum, *CM-I* Chiari malformation type I, *CM-II* Chiari malformation type II

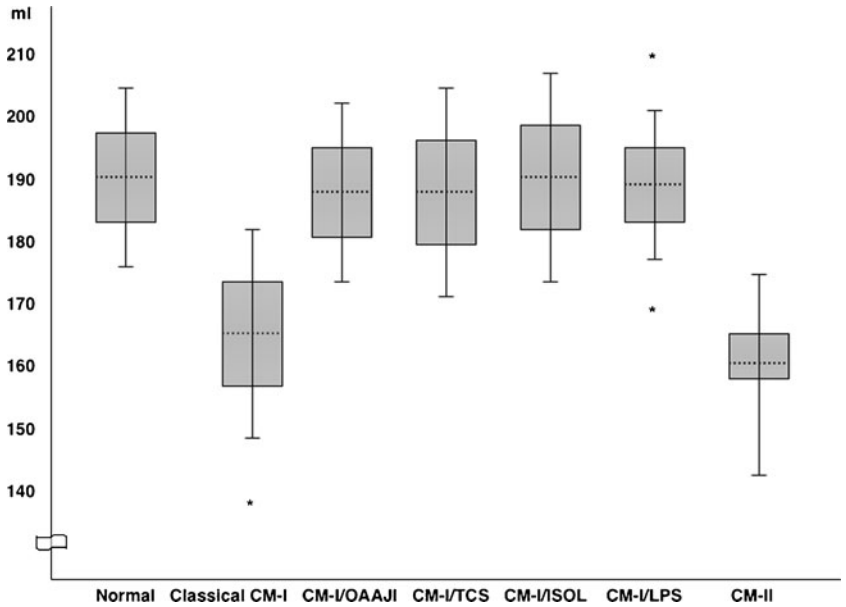

Fig. 2 Ranges of PCFV in patients with Chiari malformations stratified by etiology. In patients with CM-I, means are shown by *dotted lines*; 1 SD ranges are shown by *boxes*, and 2 SD ranges are shown by *whiskers*. In patients with CM-II, the median is shown by *dotted line*; the interquartile range is shown by *box*, and the maximum/minimum ranges are shown by *whiskers* owing to non-Gaussian distribution. *Asterisks* indicate three patients with PCFV measurements greater than 2 SD. Chiari subgroups with less than ten patients are not represented. Abbreviations: *CM-I* Chiari malformation type I, *OAAJI* occipitoatlantoaxial joint instability, *TCS* tethered cord syndrome, *ISOL* intracranial space-occupying lesions, *LPS* lumboperitoneal shunt, *CM-II* Chiari malformation type II

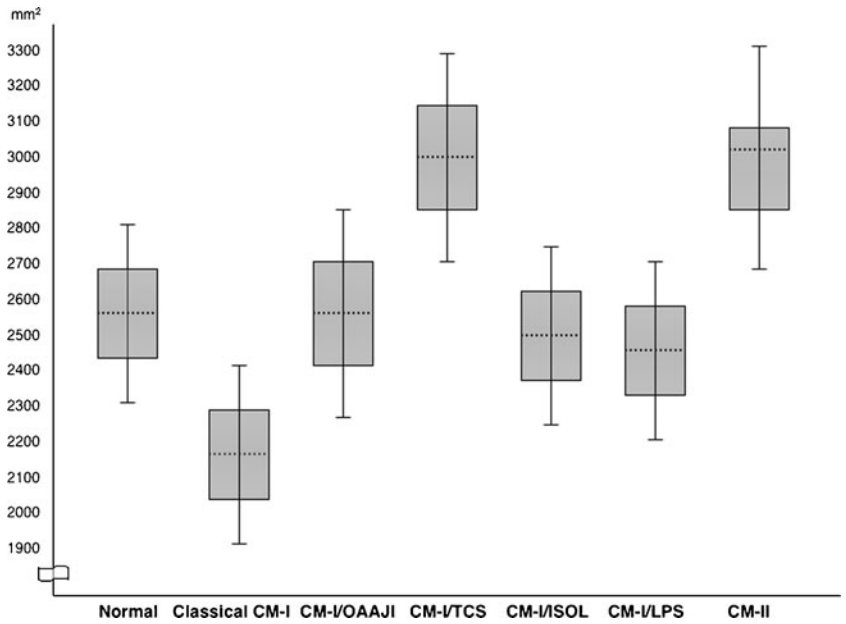

Fig. 3 Ranges of summated inferior and superior foramen magnum outlet areas stratified by etiology. In patients with CM-I, means are shown by *dotted lines*, 1 SD ranges are shown by *boxes*, and 2SD ranges are shown by *whiskers*. In patients with CM-II, the median is shown by *dotted line*; the interquartile range is shown by *box*, and the maximum/minimum ranges are shown by *whiskers* owing to non-Gaussian distribution. Chiari subgroups with less than ten patients are not represented. Abbreviations: *CM-I* Chiari malformation type I, *OAAJI* occipitoatlantoaxial joint instability, *TCS* tethered cord syndrome, *ISOL* intracranial space-occupying lesions, *LPS* lumboperitoneal shunt, *CM-II* Chiari malformation type II

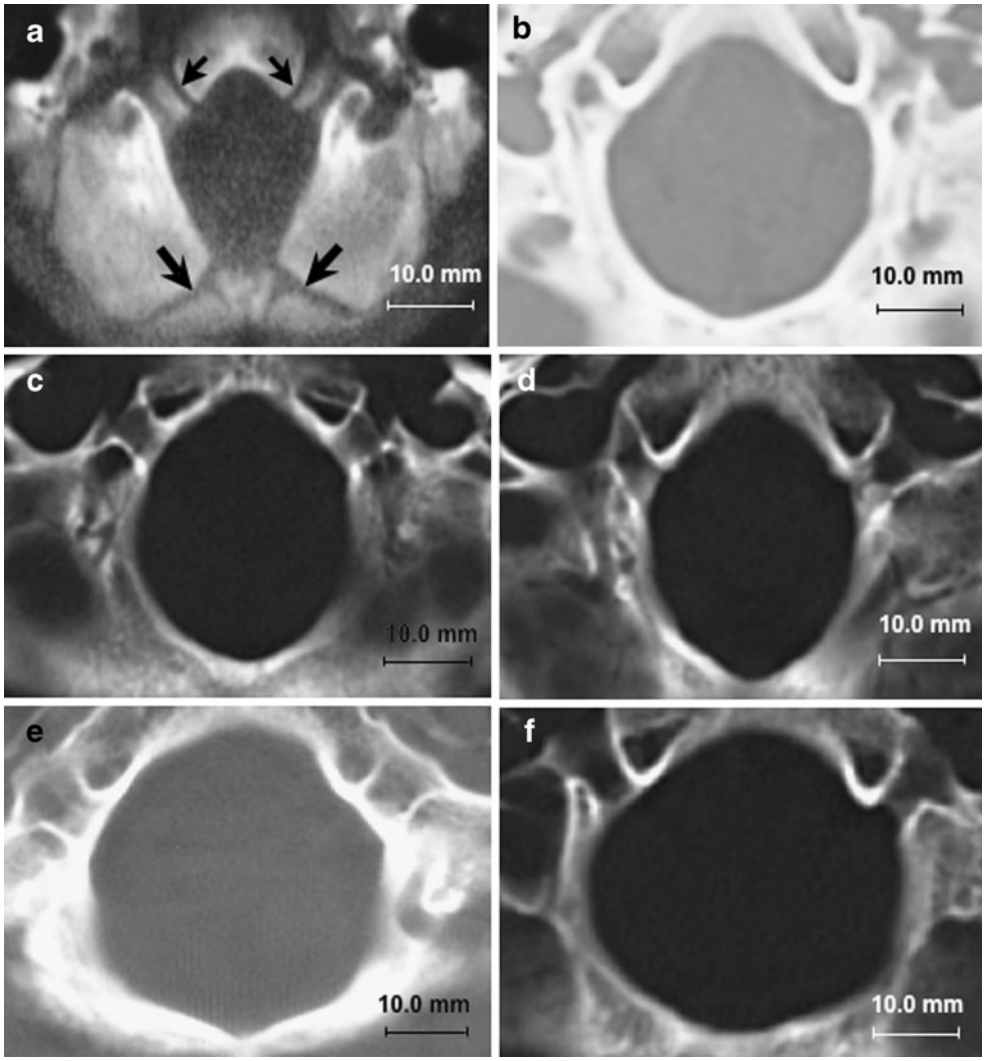

Fig. 4 Morphometric assessments of foramen magnum at level of superior outlet using axial CT images. **a** Normal foramen magnum in 10-month-old male showing patent basi-exoccipital (*small arrows*) and exosupraoccipital synchondroses (*large arrows*). **b** Normal foramen magnum in 30-year-old female with anterior–posterior diameter of 34.2 mm, transverse diameter of 31.0 mm, and area of 1,872.4 mm^2. **c** Abnormally small foramen magnum in 28-year-old female with classical CM-I. There are significant reductions of the transverse diameter (25.2 mm) and area (1,187.5 mm^2). The anterior–posterior diameter is normal giving the foramen magnum an exaggerated oval shape. **d** Abnormally small foramen magnum in 25-year-old female with CM-I and craniosynostosis (Crouzon's disease). There are significant reductions of the transverse diameter of the foramen magnum (24.8 mm) and area (1,185.4 mm^2). The anterior–posterior diameter is normal giving the foramen magnum an exaggerated oval shape. **e** Abnormally large foramen magnum in 27-year-old female with CM-I and tethered cord syndrome. There are significant increases of the anterior–posterior diameter (40.5 mm), transverse diameter (35.1 mm), and area (2,084.7 mm^2) giving the foramen magnum a rounded shape. **f** Abnormally large foramen magnum in 17-year-old male with CM-II. There are significant increases of the anterior–posterior (37.5 mm), transverse diameter (37.1 mm), and area (2,087.7 mm^2) giving the foramen magnum a rounded shape. Abbreviations: *CM-I* Chiari malformation type I, *CM-II* Chiari malformation type II

compared with healthy control individuals. PFBV was normal.

Discussion

In 752 patients with Chiari malformations, morphometric assessments of the PCF were correlated with etiological factors as a means for examining causal mechanisms of CTH. We identified 388 patients with CM-I and no associated etiological cofactors in whom the PCF was characteristically small with increasing constriction inferior to Twining's line. The FM was constricted transversely, and there was marked reduction of the inferior and superior outlet areas (see Fig. 4c, d). Above Twining's line, the PCF was slightly enlarged. Taken together, these findings appear to be consistent with premature stenosis of the basi-exoccipital and exosupraoccipital synchondroses (see

Fig. 4a), which permit lateral expansion of the FM with somatic growth [9]. Focal stenosis of the basal sutures with compensatory expansion superiorly could explain the cone-like shape of the PCF. Reductions of PCF size and volume were also present in a small number of patients with Crouzon's syndrome, Apert's syndrome, nonsyndromic craniosynostosis, achondroplasia, acromegaly, and Paget's disease. Although stenosis of the FM has been reported in association with achondroplasia [11], the reductions of PCFV reported here were more generalized than in classical CM-I, indicating different disease processes. Regardless, like classical CM-I, the presence of an abnormally small PCF suggests that cranial constriction was the most likely cause of CTH.

There were no significant abnormalities of occipital bone size, PCFV, or size and area of the FM in patients with hydrocephalus, intracranial mass lesions, OAAJI and cranial settling, and prolonged lumboperitoneal shunting. This excluded cranial constriction as the cause of CTH and directed attention to alternative mechanisms. In patients with hydrocephalus and intracranial mass lesions, there is presumptive evidence of raised intracranial pressure with attendant risk of compartmental shifts and rostral–caudal brain displacements [26]. Interestingly, Chiari's original description of CM-I was attributed by the author to "cerebellar coning" which he observed at autopsy in 14 patients dying of hydrocephalus [4]. A similar mechanism of CTH can occur in patients with infratentorial cysts and tumors, cerebellar hemorrhage, and large supratentorial mass lesions [18, 26]. In patients with OAAJI, the primary mechanism of CTH appears to be cranial settling [20]. Vivid evidence of gravitational descent of the cerebellar tonsils is sometimes provided by upright MRI [20]. In patients undergoing prolonged lumboperitoneal shunting, overdrainage of CSF is thought to create a pressure differential between the cranial and spinal compartments that draws or "sucks" the cerebellar tonsils downward. Ligation or removal of the shunt may lead to resolution of CM-I [5]. Intraspinal hypotension has also been implicated as a possible cause of CTH in patients with spinal CSF leaks, dural ectasias, and myelodysplasia [2, 18, 20].

Morphometric analysis of the PCF revealed pathological enlargement of the FM in two Chiari subgroups: (1) CM-II and (2) CM-I occurring with TCS (see Fig. 4e, f). This finding suggests that tonsillar impaction of the FM may have been present early in development before the foraminal sutures had closed. Given the complex pathology of CM-II, the cause or causes of CTH remain unknown. Proposed pathogenic mechanisms include: a lesion occurring with the primary neuroectodermal defect [3, 18], spinal cord tethering by the caudally fixed myelomeningocele [10, 15], hydrocephalus [4], or CSF leakage from the open neural tube [17]. While there is evidence for and against each hypothesis, the possibility that spinal cord tethering may play a role is supported by the observation that early postnatal repair of myelomeningocele can result in significant ascent of the cerebellar tonsils [23]. More recently, CTH has been linked to TCS in occasional patients with atypical CM-I in whom the size and volume of the PCF are normal [19]. Supporting this hypothesis are reports of increasing descent of the cerebellar tonsils with somatic growth [1], cerebellar prolapse following Chiari decompression surgery [19], and anatomical improvements including ascent of the conus medullaris, ascent of the cerebellar tonsils, and resolution of brain stem elongation following section of the FT [19]. The observation in the current study that enlargement of the FM is a pathological feature common to both CM-II and atypical cases of CM-I occurring with TCS provides additional evidence, but does not prove, that spinal cord tethering is a distinct mechanism of CTH. Table 4 classifies Chiari malformations according to presumed mechanisms of pathogenesis.

From a diagnostic standpoint, morphometric analysis of the PCF was found to be a useful supplement to the neuroradiological assessment of Chiari malformations. The analysis is easy to perform and can be made in a matter of minutes on standard MR and CT images using computer software. An important diagnostic distinction is whether the PCF is hypoplastic or normal in size. Evidence of an abnormally small PCF confirms the expected pathology and points to cranial constriction as the most likely cause of CM-I. If the size and volume of the PCF are normal,

Table 4 Mechanisms of cerebellar tonsil herniation

Cranial constriction	Spinal cord tethering	Cranial settling	Intracranial hypertension	Intraspinal hypotension
Chiari malformation type I	Tethered cord syndrome	HDCT with OAAJI	Hydrocephalus	Prolonged LPS
Craniosynostosis	Chiari malformation type II	Posttraumatic OAAJI	PCF cysts, tumors	CSF leaks
Achondroplasia		Osteogenesis imperfecta	Subdural hematoma	Dural ectasia
Acromegaly			Intracranial mass lesions	
Paget's disease				

Abbreviations: *OAAJI* occipitoatlantoaxial joint instability, *HDCT* hereditary disorders of connective tissue, *LPS* lumboperitoneal shunt, *PCF* posterior cranial fossa, *CSF* cerebrospinal fluid

however, additional evidence is required to investigate alternative mechanisms of CTH such as cranial settling, spinal cord tethering, raised intracranial pressure, and intraspinal hypotension. Morphometric analysis of the FM was also found to be helpful in the differential diagnosis of CTH by demonstrating foraminal enlargement in patients with TCS and CM-II and foraminal stenosis in patients with classical CM-I, craniosynostosis, and miscellaneous disorders such as achondroplasia.

To date, the management of patients with Chiari malformations has not been standardized. It is generally assumed but rarely proven that patients undergoing decompressive surgery have a small PCF. This assumption seems questionable given the findings reported here and raises the possibility that some outcome failures may be the result of misdiagnosis. We recommend that future neuroradiological reports include a brief description of PCF morphology to assist clinicians in the differential diagnosis of CTH.

Conclusions

The term Chiari malformation, as currently defined, embraces a heterogeneous group of disorders with different pathogenetic origins. Morphometric analysis of the PCF is required to distinguish clinical cases occurring with a pathologically small PCF from those in which the size and volume of the PCF are normal. When correlated with clinical findings, morphometric assessments of the PCF provide useful clues about the following mechanisms of CTH: (1) cranial constriction; (2) spinal cord tethering; (3) cranial setting; (4) intracranial hypertension; and (5) intraspinal hypotension. The differential diagnosis of CTH is likely to inform management strategies.

Acknowledgments We are grateful for the valuable comments by Marcus Stoodley, BMedSc, MB BS, PhD, FRACS (Professor of Neurosurgery, Australian School of Advanced Medicine, Macquarie University, New South Wales, Australia), Victor M. Haughton, MD (Director of Neuroradiology, University of Wisconsin, WI, USA), and Yuichi Inoue, MD (Professor and Chairman of Radiology, Osaka City University Graduate School of Medicine, Osaka, Japan).

Competing interests None

Ethics approval Ethics approval was provided by the Institutional Review Board of the North Shore-Long Island Jewish Health System, NY, USA. The study analyzed a deidentified set of patients in the Repository for Clinical Research in Chiari Malformation and Related Disorders (IRB #09-065).

Support Funding for the study was provided by the Research Foundation of the North Shore-Long Island Jewish Health System, NY, USA, and a grant from the Column of Hope Chiari and Syringomyelia Research Foundation, NY, USA. The work was done at the Feinstein Institute for Medical Research, which received a proportion of its funding from the National Institute of Neurological Diseases and Stroke (NINDS), NIH, MD, USA.

References

1. Abel TJ, Chowdhary A, Gabikian P, Ellenbogen RG, Avellino AM (2006) Acquired Chiari malformation type I associated with a fatty terminal filum. Case report. J Neurosurg 105:329–332
2. Atkinson JL, Weinshenker BG, Miller GM, Piegras DG, Mokri B (1998) Acquired Chiari I malformation secondary to spontaneous spinal cerebrospinal fluid leakage and chronic intracranial hypotension syndrome in seven cases. J Neurosurg 88:237–242
3. Barry A, Patten BM, Stewart BH (1957) Possible factors in the development of the Arnold–Chiari malformation. J Neurosurg 14:285–301
4. Chiari H (1891) Über Veränderungen des Kleinhirns in folge von Hydrocephalie des Grosshirns. Dtsch Med Wochenschr 17:1172–11725
5. Chumas PD, Armstrong DC, Drake JM, Kulkarni AV, Hoffman HJ, Rutka HRP, JT HEB (1993) Tonsillar herniation: the rule rather than the exception after lumboperitoneal shunting in the pediatric population. J Neurosurg 78:568–573
6. Cinalli G, Spennato P, Sainte-Rose C, Arnaud E, Aliberti F, Brunnelle F, Cianciulli E, Renier D (2005) Chiari malformation in craniosynostosis. Childs Nerv Syst 21:889–901
7. Elisevich K, Fontaine S, Bertrand G (1987) Syringomyelia as a complication of Paget's disease. Case report. J Neurosurg 66:611–613
8. Elster AD, Chen MY (1992) Chiari I malformations: clinical and radiologic reappraisal. Radiology 183:347–353
9. Friede H (1981) Normal development and growth of the human neurocranium and cranial base. Scand J Plast Reconstr Surg 15:163–169
10. Goldstein F, Kepes JJ (1966) The role of traction in the development of the Arnold–Chiari malformation. An experimental study. J Neuropathol Exp Neurol 25:654–666
11. Jha RM, Klimo P, Smith ER (2008) Foramen magnum stenosis from overgrowth of the opisthion in a child with achondroplasia. J Neurosurg Pediatrics 2:36–38
12. Lee M, Rezai AR, Wisoff JH (1995) Acquired Chiari-I malformation and hydromyelia secondary to a giant craniopharyngioma. Pediatr Neurosurg 22:251–254
13. Lemar HJ Jr, Perloff JJ, Merenich JA (1994) Symptomatic Chiari-I malformation in a patient with acromegaly. South Med J 87:284–285
14. Lew SM, Kothbauer KF (2007) Tethered cord syndrome: an updated review. Pediatr Neurosurg 43:236–248
15. Lichtenstein BW (1942) Distant neuroanatomic complications of spina bifida (spinal dysraphism). Hydrocephalus, Arnold–Chiari deformity, stenosis of the aqueduct of Sylvius, etc.; pathogenesis and pathology. Arch Neurol Psychiatry 47:195–214

16. Mayhew TM, Olsen DR (1991) Magnetic resonance imaging (MRI) and model-free estimates of brain volume determined using the Cavalieri principle. J Anat 178:133–144
17. McLone DG, Knepper PA (1989) The cause of Chiari II malformation: a unified theory. Pediatr Neurosci 15:1–12
18. Milhorat TH (1978) Pediatric neurosurgery. Contemporary neurology series. FA Davis, Philadelphia, PA
19. Milhorat TH, Bolognese OA, Nishikawa M, Francomano CA, McDonnell NB, Roonprapunt C, Kula RW (2009) Association of Chiari malformation type I and tethered cord syndrome: preliminary results of sectioning filum terminale. Surg Neurol 72:20–35
20. Milhorat TH, Bolognese PA, Nishikawa M, McDonnell NB, Francomano CA (2007) Syndrome of occipitoatlantoaxial hypermobility, cranial settling, and Chiari malformation type I in patients with hereditary disorders of connective tissue. J Neurosurg Spine 7:601–609
21. Milhorat TH, Chou MW, Trinidad EM, Kula RW, Mandell M, Wolpert C, Speer MC (1999) Chiari I malformation redefined: clinical and radiographic findings for 364 symptomatic patients. Neurosurgery 44:1005–1017
22. Morioka T, Shono T, Nishio S, Yoshida K, Hasui K, Fukui M (1995) Acquired Chiari I malformation and syringomyelia associated with bilateral chronic subdural hematoma. Case report. J Neurosurg 83:556–558
23. Morota N, Ihara S (2008) Postnatal ascent of the cerebellar tonsils in Chiari malformation type II following surgical repair of myelomeningocele. J Neurosurg Pediatrics 2:188–193
24. Müller F, O'Rahilly R (1994) Occipitocervical segmentation in staged human embryos. J Anat 185:251–258
25. Nishikawa M, Sakamoto H, Hakuba A, Nakanishi N, Inoue Y (1997) Pathogenesis of Chiari malformation: a morphometric study of the posterior cranial fossa. J Neurosurg 86:40–47
26. Plum F, Posner JB (1966) Diagnosis of stupor and coma. Contemporary neurology series. FA Davis, Philadelphia, PA
27. Pyeritz RE (2000) Ehlers-Danlos syndrome. N Engl J Med 342:730–732
28. Rinaldi F, Cioffi FA, Columbano L, Krasagakis G, Bernini FP (2005) Tethered cord syndrome. J Neurosurg Sci 49:131–135
29. Schaefer GB, Thompson JN Jr, Bodensteiner JB, Gingold M, Wilson M, Wilson D (1991) Age-related changes in the relative growth of the posterior fossa. J Child Neurol 6:15–19
30. Stovner LJ, Bergan U, Nilsen G, Sjaastad O (1993) Posterior cranial fossa dimensions in the Chiari I malformation: relation to pathogenesis and clinical presentation. Neuroradiology 35:113–118

Comments

This article represents an enormous experience of the management of cerebellar tonsillar ectopia.The conclusion that tonsillar herniation is aetiologically heterogeneous is an important one and the recommendation to consider aetiology in the planning of management entirely valid.

It is in suggesting a potential aetiological association between tethered cord (in this publication the mildest form of tethering - fatty filum terminale) and tonsillar herniation that the article is perhaps most controversial particularly having used measurements from cases of Chiari II malformation as evidence to support this assertion. The Chiari II malformation, as pointed out by the authors is a pathologically distinct entity almost exclusively found in the context of neural tube defects. It is a primary defect of the CNS parenchyma, tonsillar herniation being only one component of a much more extensive hindbrain malformation. Inclusion of Chiari II patients in this study detracts from the hypothesis being tested.

Are we to assume that the traction generated through the whole spinal cord by a 2mm thick filum on a slightly low conus, is responsible for herniation of the cerebellar tonsils, particularly remembering that the spinal cord is of course not free floating in a spinal column of CSF but itself attached to its dural container for almost all its length via the dentate ligaments? If this were to be the case should not tonsillar herniation be an almost ubiquitous finding in the more severe dysraphic states such as lipomyelocele? Most neurosurgeons distinguish the modest 5mm descent of the cerebellar tonsils from cases where the tonsils extend to C2 or beyond. It would be helpful to know how the severity of the herniation varied between the subgroups in this study. Both fatty filum terminale and mild tonsillar descent are common incidental neuroradiological observations and their occasional coexistence may be little more than serendipidous. The hypothesis presented is provocative and the potential clinical implications significant..... all the more reason for the supporting evidence to be more robust.

Dominic Thompson
London, UK